Journal of Alloys and Compounds 504 (2010) 123–128

Contents lists available at ScienceDirect

Journal of Alloys and Compounds

journal homepage: www.elsevier.com/locate/jallcom

Effect of ZnO whisker content on sinterability and fracture behaviour of PZT peizoelectric composites

Jie Yuan[a,1], Da-Wei Wang[b,1], Hai-Bo Lin[b], Quan-Liang Zhao[b], De-Qing Zhang[b], Mao-Sheng Cao[b,*]

[a] School of Information Engineering, Central University for Nationalities, Beijing 100081, China
[b] School of Materials Science and Engineering, Beijing Institute of Technology, Beijing 100081, China

ARTICLE INFO

Article history:
Received 14 November 2009
Received in revised form 16 May 2010
Accepted 21 May 2010
Available online 31 May 2010

Keywords:
Composite materials
PZT/ZnO_w
Sintering
Mechanical properties

ABSTRACT

Zinc oxide whiskers (ZnO_w) reinforced lead zirconate titanate (PZT) piezoelectric composites with high strength and high toughness were fabricated by nonpressure sintering at 1100 °C. Addition of ZnO_w is effective for sinterability and densification of the composites. Incorporating ZnO_w to PZT ceramics contributes to an obvious improvement of the fracture properties. The fracture strength and fracture toughness of the composites incorporating 2 wt.% ZnO_w, compared with the monolithic PZT, are enhanced 46% and 47%, respectively. Improvement of fracture strength is ascribed to the enhancement of the elastic modulus and fracture toughness. Enhancement of fracture toughness is associated with the existence of the observed several mechanisms including crack deflection, whisker bridging, whisker pull-out and rupture due to the intergranular and intragranular whiskers.

1. Introduction

Lead zirconate titanate (PZT) piezoelectric ceramics exhibit excellent piezoelectric and dielectric properties and are widely applied in numerous electronic devices, such as actuators, sensors, capacitors, resonators, and high-power transducers [1–7]. On the other hand, PZT ceramics have been extensively modified with different additives, which make them more attractive for specific applications [8–14]. With the miniaturization and integration of electronic circuits, small-scale piezoelectric devices are technologically important in the fields of smart materials and microelectromechanical systems (MEMS) [15]. However, the piezoelectric ceramics suffer from low mechanical strength and the resulting low reliability on the performance of the devices under severe circumstances.

The concept of a functionally graded material (FGM) has been used to overcome this problem. Piezoelectric ceramic/ceramic FGMs were studied to reduce the interfacial stress concentration in the actuator [16,17]. However, the corresponding mechanical properties of ceramic/ceramic composites have not been enhanced effectively due to the brittle nature. Several approaches to improve mechanical properties have been used to investigate the composites incorporating polymers, metals, fibers or whiskers [18–28]. PZT piezoelectric ceramic based composites incorporating polymers were developed to improve the mechanical properties by sacrificing the dielectric properties sharply [27]. The addition of metal particles stimulates the graded piezoelectric properties and the improvement of the mechanical properties [15,19], whereas both Pt and Ag noble metals are too expensive to be suitable candidates for practical applications. Recently, increasing attention has been paid to whisker-reinforced ceramics. Whisker/fiber-reinforced ceramic matrix composites reveal the substantial improvements in strength and toughness of the matrix and the distributed whiskers as bridges can resist crack growth because the energy of cracks may be dissipated at the whisker/matrix interface [29,30]. Silicon carbide whiskers (SiC_w) have been extensively investigated on the reinforcement for composites because of their ability to reinforce brittle ceramics [31]. SiC_w reinforced PZT ceramic composites have shown excellent mechanical properties except the electrical properties [32]. There are, however, limited reports on the PZT ceramic matrix composites by the addition of ZnO whiskers (ZnO_w). Practically until now, it is significant to discover the interesting and distinctive piezoelectric, semiconducting properties in the ZnO nanostructures for nanogenerator applications and microelectric devices. In addition, ZnO nanostructures have received considerable attention on potential applications of the specific electrical, optoelectronic and microwave absorption properties for several decade years [33–43]. In our previous works, we selected ZnO_w as the second phase to adjust both the electrical and the mechanical properties of piezoelectric composites [44–47]. Due to the high-temperature strength, rigidity and chemical stability, ZnO_w have been a subject of intensive research as reinforced composite materials [48,49]. Among them, a variety of reinforcements with different morphologies have

* Corresponding author. Tel.: +86 10 68914062.
E-mail address: caomaosheng@bit.edu.cn (M.-S. Cao).
[1] These authors contributed equally to this work.

0925-8388/$ – see front matter © 2010 Elsevier B.V. All rights reserved.
doi:10.1016/j.jallcom.2010.05.067

met different degrees of success. Furthermore, the doping effect of ZnO powder in piezoelectrics can result in lower sintering temperature and improving electric properties [50–54] and the PZT/ZnO actuator sensitive to reducing gases was fabricated [55].

In the present study, high strength and high toughness PZT-based composites incorporating ZnO_w were fabricated by non-pressure sintering. A purpose is to investigate the effects of ZnO_w content on the sinterability and fracture behaviour in a compositional range from 1 to 10 wt.% ZnO_w content.

2. Experimental procedures

Commercially available ceramic powders of $Pb(Zr,Ti)O_3$ (PZT-5MN, Hongsheng Industry, Baoding, China) with composition in the morphotropic phase boundary were used as the raw materials. ZnO_w were synthesized by the conventional growth process involving vapor phase oxidation of fine zinc powders (purity 99.999%). Detailed fabrication procedures of ZnO_w were described in a previous paper [35]. The as-prepared ZnO_w were added to the PZT matrix in the range 1–10 wt.% and then ball milled for 24 h with zirconia balls as the grinding media and alcohol as the solvent (during the ball-milling process, part of the ZnO_w could be destroyed and broken into the needle-like ZnO nanostructures, which can serve as the reinforced material just like the short fibers). After milling, the slurry was dried at room temperature. These powders were dispersed in an agate mortar with an appropriate amount of polyvinyl alcohol solution as a binder. The mixtures were dried, sieved and then uniaxially pressed into disc shape under a pressure of 200 MPa. The green bodies were sintered regularly in a covered alumina crucible containing $PbZrO_3$ powders to minimize PbO evaporation. The sintered bodies sintered at 1100 °C for 2 h were machined to the required dimensions and sized from the bulk for property measurements.

The bulk density was measured by the Archimedes method in distilled water, and the relative density was calculated using the theoretical density. The samples were machined into bars of 36 mm × 4 mm × 3 mm to measure the fracture strength by the three-point bending method with a span of 30 mm and a cross-head speed of 0.5 mm/min, at room temperature in air. Single-edge notched-beam (SENB) specimens were fabricated by notching the segments of tested flexure specimens. For the fracture toughness K_{IC}, the 24 mm × 4 mm × 2 mm SENB samples were tested in three-point loading with a span of 20 mm and a cross-head speed of 0.05 mm/min. The crystal structures of the sintered composites were examined by the X-ray diffraction (XRD) with Ni-filtered Cu $K\alpha$ radiations. The microstructures and fracture surfaces of the specimens were observed by a scanning electronic microscope (SEM). For electrical measurement, both sides of the sintered pellets were polished, painted with silver paste and fired at 800 °C for 10 min. The dielectric and electromechanical characteristics were measured with a Model HP 4194 impedance analyzer. Poling treatment was carried out in silicon oil at 120 °C for 20 min with an electric field of 3–4 kV/mm prior to the piezoelectric constant measurement using a ZJ-3AN piezoelectric tester.

3. Results and discussion

Fig. 1(a) shows the typical morphology of ZnO_w synthesized by the simple combustion oxidation method. The products consist of abundant tetra-needle-like ZnO_w with uniform structure. The typical microstructure of the polished surface for the PZT/ZnO_w composite samples with 5 wt.% ZnO_w sintered at 1100 °C for 2 h are shown in Fig. 1(b). The dark phases are ZnO_w, which are homogeneously dispersed in the gray phases PZT. The phase compatibility between the PZT and ZnO_w appears to be good at the processing temperatures of 1100 °C.

The XRD patterns of the monolithic PZT and PZT/ZnO_w composites with various amounts of ZnO_w addition are shown in Fig. 2. From the assigned PZT and ZnO phases in the patterns, the PZT perovskite phase and ZnO phase are retained after the sintering process. XRD patterns also confirm that there is no significant chemical reaction occurring between the PZT and ZnO_w in the composites during sintering at 1100 °C. The diffraction intensities of ZnO peaks increase slightly with the increasing ZnO_w content, indicating that the PZT matrix is a phase compatible with ZnO_w content. Thus, the "co-existence" of the matrix and the whisker during the sintering temperature is achieved. Furthermore, it is clear that the single peak between 40° and 50° from the PZT began to split into two peaks with the addition of ZnO_w, indicating that the phase structure of PZT changed from rhombohedral phase to tetragonal phase

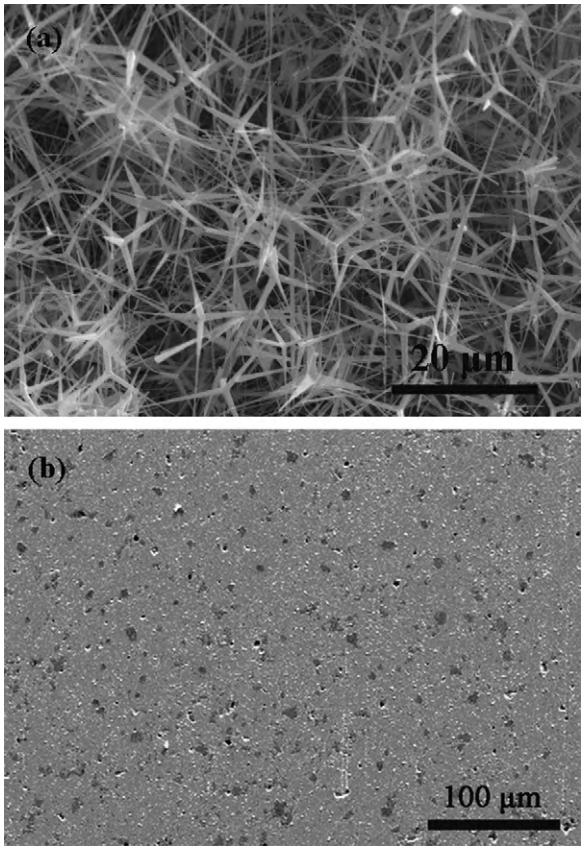

Fig. 1. SEM micrograph of the typical microstructure of (a) ZnO whiskers and (b) the PZT/5 wt.% ZnO_w composite sintered at 1100 °C.

[54], which is suggested that Zn^{2+} ions in ZnO enter B site of the PZT lattice, partially replace Zr^{4+}/Ti^{4+} ions because of the proximity of their ionic radius [52] and change the crystal structure of PZT.

The relative density of the monolithic PZT and PZT/ZnO_w composites as a function of the various amounts of ZnO_w is shown

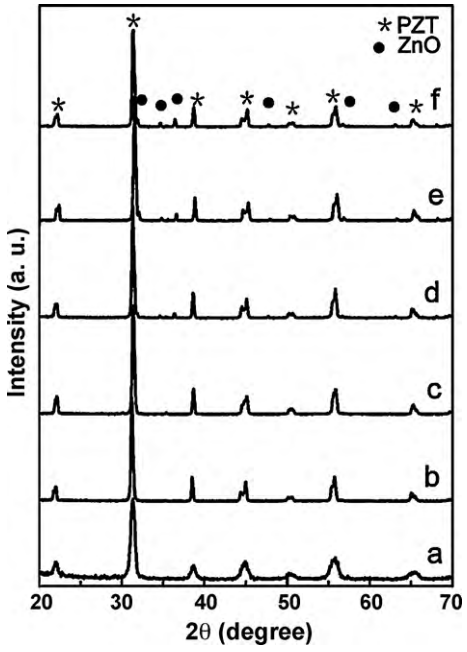

Fig. 2. XRD patterns of (a) the monolithic PZT and PZT/ZnO_w composites with (b) 1 wt.%, (c) 2 wt.%, (d) 5 wt.%, (e) 8 wt.% and (f) 10 wt.% ZnO_w.

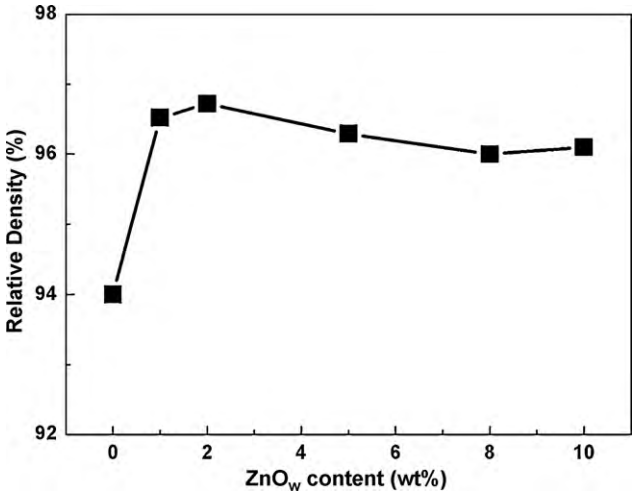

Fig. 3. Effect of the ZnO_w content on the relative density of PZT/ZnO_w composites sintered at 1100 °C/2 h.

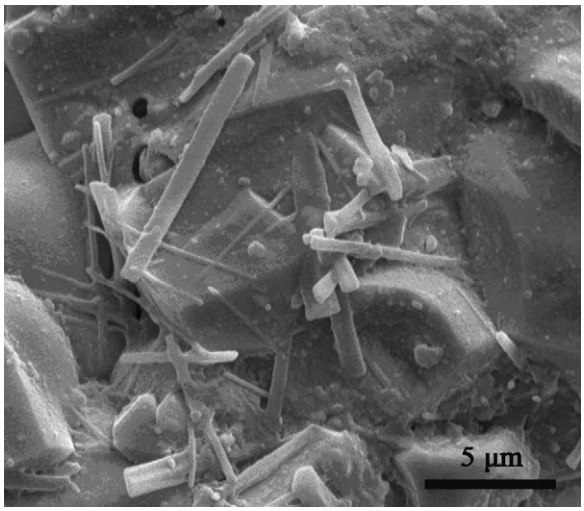

Fig. 4. SEM micrograph of the fracture surface of the PZT/2 wt.% ZnO_w composite.

in Fig. 3. The relative density of the monolithic PZT ceramics sintered at 1100 °C is lower than 95%, whereas all the composites with the addition of ZnO_w are obtained more than 96% of the theoretical density value sintered at 1100 °C. The curve indicates that the densification rate is improved sharply after the incorporation of ZnO_w. For the composites, the relative density increases with the ZnO_w addition. Therefore, incorporation of ZnO_w exhibits significant effect on the densification and the sinterability of the PZT composites is effectively accelerated by a small quantity of ZnO_w. The addition of ZnO_w makes it possible to reduce the sintering temperature to achieve low-temperature sintering of PZT ceramics with high densification.

A previous study on the PZT-based composites reinforced by SiC_w indicated that the porosity increased and the sintered density decreased with the increasing SiC_w content [31]. This phenomenon of the SiC_w addition is not a coincidence with the result of the ZnO_w contribution. Compared with the thermal expansion coefficient (CTE) of PZT, due to the CTE of ZnO_w with a difference smaller than that of SiC_w, it is expected that little amounts of residual stresses can be introduced into matrix grains and ZnO_w during the sintering process. There is a probable mechanism responsible for the low-temperature sintering observed in the PZT/ZnO_w composites, consistent with other PZT-based ceramics containing ZnO powder [50–52]. Since material transfer in the liquid phase is much faster than that in the solid state, the formation of liquid phase sintering is promoted by the ZnO addition and increases with the increasing ZnO content. Microstructure analysis reveals that the liquid phase along the grain boundary partially appears with addition of ZnO_w at the sintering temperature of 1100 °C, as shown in Fig. 4. Therefore, these results indicate that either ZnO whisker or powder can help the sintering of the specimens at a low temperature.

Fig. 5 shows the dependence of the fracture strength and fracture toughness of the PZT/ZnO_w composites on the ZnO_w content. The fracture strength increases with the amount of ZnO_w up to 2 wt.% and then decreases with further increase of the ZnO_w amount. The fracture toughness is improved upon increasing the content of ZnO_w from 0 to 2 wt.%, but further addition of ZnO_w results in a drastic decrease in fracture toughness. It should be noted that the highest fracture strength and fracture toughness are obtained for PZT/ZnO_w with the addition of 2 wt.% ZnO_w. The fracture strength of 98 MPa and fracture toughness of 1.44 MPa $m^{1/2}$ for the PZT/2 wt.% ZnO_w composites are about 146% and 147% that of the ZnO_w-free PZT ceramics, respectively. Therefore, the addition of ZnO_w effectively contributes to enhancing the fracture behaviours of the PZT/ZnO_w composites.

The improvement of the fracture strength is attributed to critical flaw size, largely depending on the average grain size, fracture toughness, and elastic modulus in the simplest manner [56]. Since the grain size of the monolithic PZT is similar to those of the composites as mentioned above, it is evident that positive effects of the fracture strength improvement for the composites can be ascribed to the enhancement of the elastic modulus and fracture toughness. ZnO_w have high elastic modulus and high strength and fit the condition $E_w > 2E_m$ (E_w is the elastic modulus of ZnO_w, $E_w \approx 350$ GPa and E_m is the elastic modulus of the PZT matrix, $E_m \approx 70$ GPa). Considering the weight fraction effect, the elastic modulus of the PZT/ZnO_w composites increases with whisker content and is much higher than that of the PZT/Ag-particle composites due to the $E_w \gg E_p$ (E_p is the elastic modulus of Ag-particle and as the same as E_m). Due to the small possibility of whisker agglomeration and the low thermal stresses before 2 wt.% ZnO_w, the strengthening effect of elastic modulus and fracture toughness can play a major role. On the other hand, with the further increase of the ZnO_w content, a negative influence on the fracture behaviours tends to be more intense. The agglomeration of ZnO_w is more likely to occur so that the bonding is loosed and the critical defect size in the composites grows. This leads to the degradation of fracture strength and fracture toughness of the composites with more ZnO_w amount. Therefore, all the difference of fracture behaviours results from the above two factors.

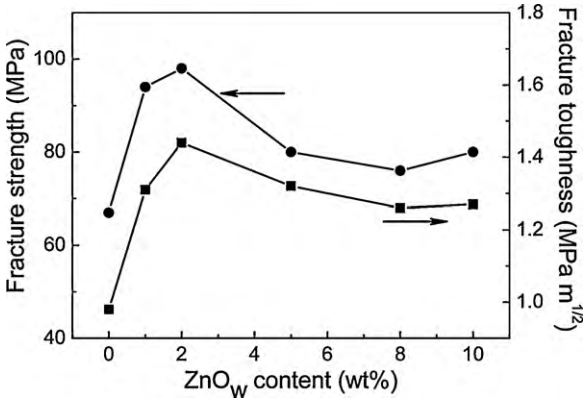

Fig. 5. Effect of ZnO_w content on the fracture strength and fracture toughness of PZT/ZnO_w composites.

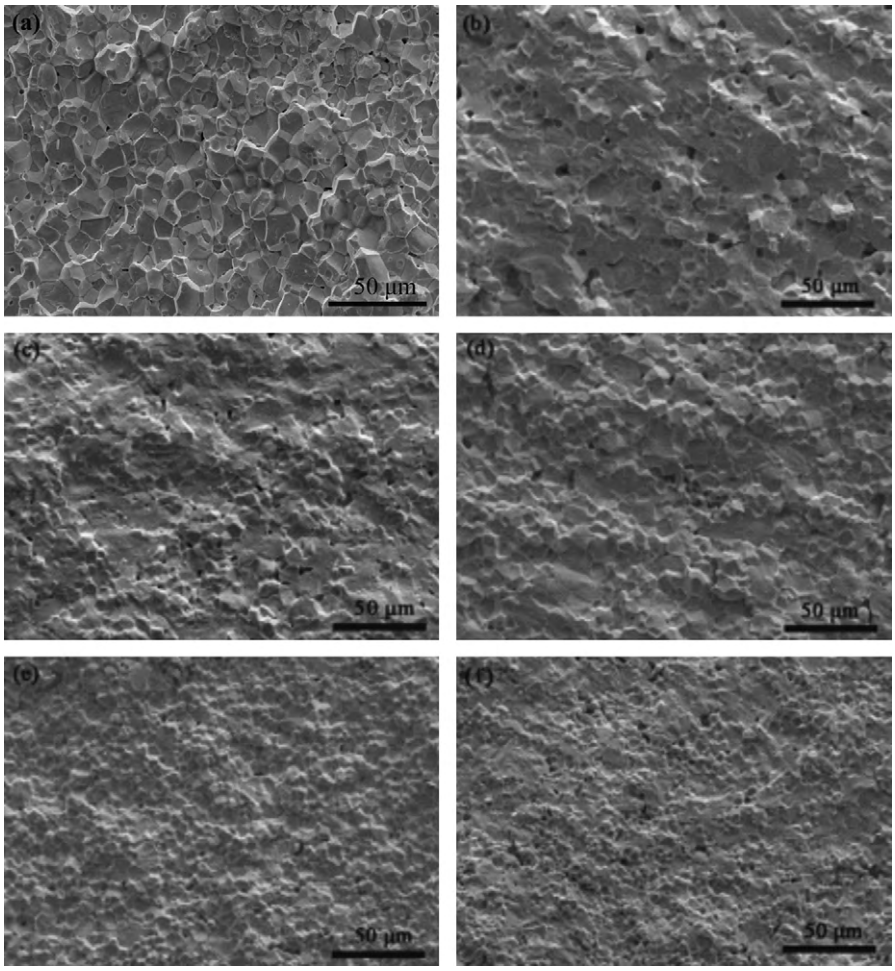

Fig. 6. SEM fractographs of fracture features on the specimens of the PZT/ZnO_w composites with (a) 0 wt.%, (b) 1 wt.%, (c) 2 wt.%, (d) 5 wt.%, (e) 8 wt.% and (f) 10 wt.% ZnO_w.

The fracture behaviour of reinforced composites is expected to characterize like their fiber/whisker-reinforced composites [23]. To seek the toughening mechanisms of reinforcement, the micrographs of fracture surface are examined to reveal the fracture mode. Fig. 6 shows the SEM photographs of the fracture surfaces of the monolithic PZT and PZT/ZnO_w composite specimens containing 1, 2, 5, 8 and 10 wt.% ZnO_w. It is observed that the grain boundaries of the monolithic PZT are very clear, resulting from its dominating intergranular fracture mode. However, the fracture surfaces of the PZT/ZnO_w composites are rougher than that of the monolithic and the roughness of the fracture surface increases with the increasing ZnO_w content. In other words, the fracture mode of the PZT/ZnO_w composites is a mixture of transgranular and intergranular modes, where the degree of intergranular fracture decreases with the increasing ZnO_w content. Furthermore, since the elastic modulus of the whisker are much larger than that of matrix, the crack tip stresses could be changed such that a crack traveling normal to the whisker axis is deflected out of plane as it approaches the whisker. Usually, the crack deflection is associated with debonding of the whisker/matrix interface which presents the weak interface strength leading to the whisker fracture behaviours [57]. Hence, in the case of the partially debonding interface of the ceramic matrix composites with discontinuous reinforcement, multiple mechanisms such as reinforcement bridging, pull-out, crack deflection could occur [58].

The whiskers could enable the cracked matrix to suspend a certain level of strength and the rupture ones could also increase the energy-absorption during fracture. Due to the debonding of the whisker–matrix interfaces, to a certain extent, the whiskers would be not broken immediately but rather have gone through a whisker–matrix interaction process as the crack front reached and passed through them. Otherwise, the whiskers would have broken along the crack plane with no holes and exposed parts observed. Hence, the bridging of matrix cracks and pull-out from matrix by the ZnO_w could also occur during the failure of the composites. Fig. 7 displays a typical micrograph of the composites where the whisker with a width of 0.5 μm bridges the matrix grains. According to the elastic fracture mechanics [59], the bridging mechanism of

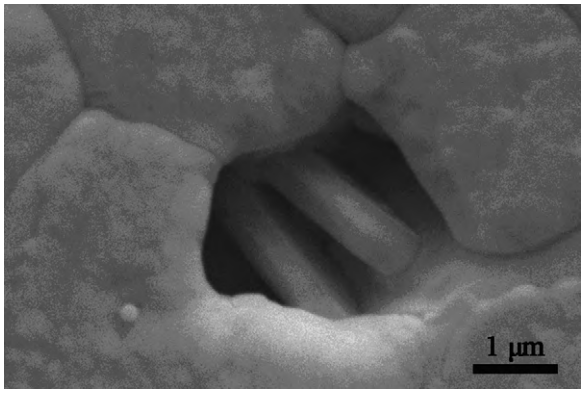

Fig. 7. SEM micrograph of the typical interaction between whisker and matrix, showing the bridging by the reinforcement phase.

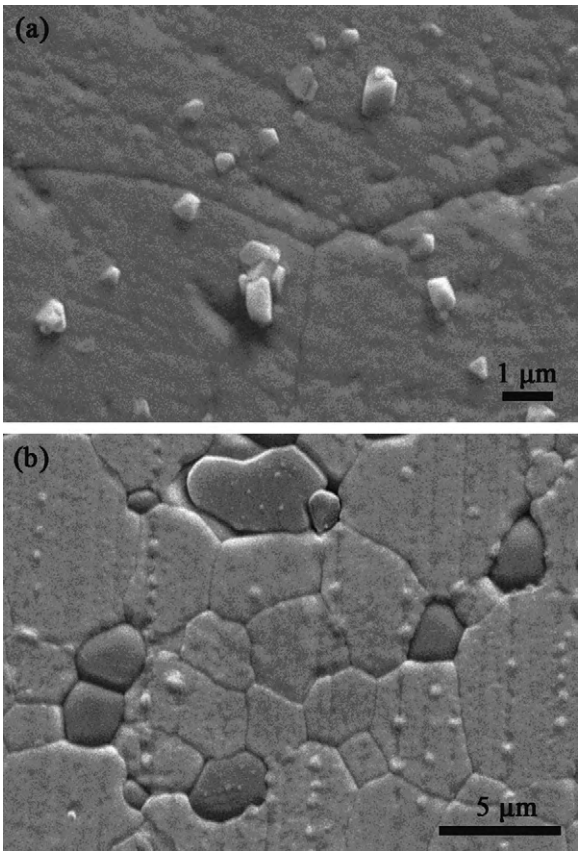

Fig. 8. Typical micrographs of the PZT/8 wt.%ZnO_w composites: (a) intragranular microstructure and (b) intergranular microstructure.

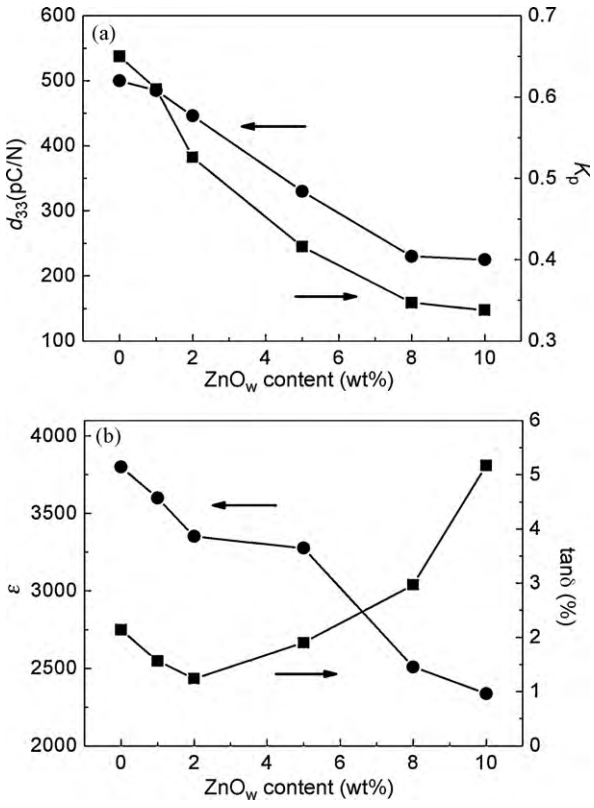

Fig. 9. Effect of ZnO_w content on the piezoelectric and dielectric properties of PZT/ZnO_w composites.

the PZT/ZnO_w composites clearly represents an intrinsically higher energy source of fracture resistance for matrix grains. During the whisker pull-out, energy that would normally cause crack propagation is partially expended by debonding and by friction as the whisker slid against adjacent microstructure features. That could effectively increase the work of fracture toughness.

The non-planar crack arises from residual stresses in the weak interface, which is attributed to the intragranular and intergranular grains [60,61]. We also find that most of the smaller scale ZnO whiskers are seated in the PZT grains as shown in Fig. 8(a), while the larger ones are located at the matrix grain boundaries seen from Fig. 8(b). The intragranular whiskers are in the size range to 500 nm and some whiskers are oriented perpendicular to the matrix plane and pull-out of the matrix (in Fig. 8(a)). The intergranular ones are in the size range 2–4 μm and some debonding interfaces between whisker and matrix are present (in Fig. 8(b)). Based on the concept of elasticity [62], the intragranular ZnO whiskers have a positive effect on the bridging and pulling-out of PZT grains because the elastic modulus of whisker is greater than that of matrix. On the other hand, the intergranular whiskers can also pin the PZT and aggregate at the grain boundaries. The propagating cracks reach the intragranular whiskers and then proceed with the whiskers pulling-out and bridging and possibly fracturing, while cracks are arrested upon reaching the intergranular whiskers from the interface and then deflected along the interface, leaving partially the whisker intact. These estimations are in agreement with the observed whiskers in the fracture surface examinations as shown in Fig. 4. In fact, under the stress conditions, the intragranular whiskers will perturb the crack tip, causing a reduction in the stress intensity. The existence of intergranular whiskers at the grain boundaries causing crack deflection could drive more fracture energy dissipated. All these cases can increase the energy absorbed during fracture. Therefore, the mechanisms of the whisker pull-out, bridging and rupture undoubtedly improve the fracture toughness of the composites, which is consistent with the mechanical properties. It is believed that these ZnO_w serve as additional reinforcement elements, which result in a contribution to the increase of fracture strength and fracture toughness.

Fig. 9 shows the dependence of the piezoelectric and dielectric properties of the PZT/ZnO_w composites on the ZnO_w content. Due to the essential low-piezoelectricity, the introduction of ZnO_w in PZT would lead to the decline of piezoelectric and dielectric properties [44]. As shown in Fig. 9(a) and (b), with the increase of ZnO_w content, the piezoelectric constant d_{33}, electromechanical coupling factor k_p and relative dielectric constant ε of the composites decline, while the dielectric loss tanδ increases greatly, which is mainly attributed to the local micro-conductance loss of the semiconductor ZnO_w.

4. Conclusions

ZnO–whisker-reinforced PZT piezoelectric composites have been fabricated by nonpressure sintering at 1100 °C. ZnO_w are homogeneously dispersed in the PZT ceramics and there are no reaction phases between the matrix PZT and ZnO_w during the sintering process. A small quantity of ZnO_w accelerates the sinterability of the PZT composites and the relative density increases with the increasing whisker content. The fracture behaviour of PZT/ZnO_w composites is obviously improved by the addition of ZnO_w. The fracture strength and fracture toughness of the PZT/2 wt.% ZnO_w composites, compared with the monolithic PZT, are enhanced about 46% and 47%, respectively. The fracture strength improvement for the PZT/ZnO_w composites is ascribed to the enhancement of the elastic modulus due to the combined effect

and fracture toughness. The incorporation of ZnO_w is effective in suppression of the crack propagation and the composites show the change from intergranular to transgranular modes of fracture. The fracture toughness enhancement is correlated to the observed several toughening mechanisms including crack deflection, whisker bridging, pull-out and rupture due to the intergranular and intragranular whiskers. These mechanisms have a significant influence on the mechanical properties of the composites.

Acknowledgements

This research is financially supported by the National Natural Science Foundation of China under Grant Nos. 50742007, 50872159 and 50972014, the National Defense Fund of China under Grant No. 401050301, the National High-Tech Research and Development Program (863 program) of China under Grant No. 2007AA03Z103, and the Key Laboratory Foundation of Sonar Technology of China under Grant No. 9140C24KF0901.

References

[1] G.H. Haertling, J. Am. Ceram. Soc. 82 (1999) 797–818.
[2] P.A. Jadhav, M.B. Shelar, B.K. Chougule, J. Alloys Compd. 479 (2009) 385–389.
[3] D.G. Liu, H.X. Zhang, W. Cai, X.W. Wu, L.C. Zhao, Mater. Chem. Phys. 51 (1997) 186–189.
[4] S.S. Chougule, D.R. Patil, B.K. Chougule, J. Alloys Compd. 452 (2008) 205–209.
[5] Z.P. Yang, H. Li, X.M. Zong, Y.F. Chang, J. Eur. Ceram. Soc. 26 (2006) 3197–3202.
[6] S.S. Chougule, B.K. Chougule, J. Alloys Compd. 456 (2008) 441–446.
[7] C.Q. Liu, W.L. Li, W.D. Fei, S.Q. Zhang, J.N. Wang, J. Alloys Compd. 493 (2010) 499–501.
[8] K. Ramam, A.J. Bell, C.R. Bowen, K. Chandramouli, J. Alloys Compd. 473 (2009) 330–335.
[9] X.L. Chao, Z.P. Yang, Y.F. Chang, M.Y. Dong, J. Alloys Compd. 477 (2009) 243–249.
[10] K. Ramam, M. Lopez, J. Alloys Compd. 466 (2008) 398–403.
[11] D.W. Wang, D.Q. Zhang, J. Yuan, Q.L. Zhao, H.M. Liu, Z.Y. Wang, M.S. Cao, Chin. Phys. B 18 (2009) 2596–2602.
[12] B.T. Liu, C.S. Cheng, F. Li, D.Q. Wu, X.H. Li, Q.X. Zhao, Z. Yan, X.Y. Zhang, J. Alloys Compd. 440 (2007) 276–280.
[13] F. Gao, R.Z. Hong, J.J. Liu, Z. Li, L.H. Cheng, C.S. Tian, J. Alloys Compd. 475 (2009) 619–623.
[14] X.L. Chao, D.F. Ma, R. Gu, Z.P. Yang, J. Alloys Compd. 491 (2010) 698–702.
[15] J.F. Li, K. Takagi, N. Terakubo, R. Watanabe, Appl. Phys. Lett. 79 (2001) 2441–2443.
[16] X.H. Zhu, Z.Y. Meng, Sens. Actuators A 48 (1995) 169–176.
[17] C.C.M. Wu, M. Kahn, W. Moy, J. Am. Ceram. Soc. 79 (1996) 809–812.
[18] J. Su, T.B. Xu, S.J. Zhang, T.R. Shrout, Q.M. Zhang, Appl. Phys. Lett. 85 (2004) 1045–1047.
[19] H.J. Hwang, K. Watari, M. Sando, M. Toriyama, K. Niihara, J. Am. Ceram. Soc. 80 (1997) 791–793.
[20] K. Tajima, H.J. Hwang, M. Sandob, K. Niihara, J. Eur. Ceram. Soc. 19 (1999) 1179–1182.
[21] Y. Bao, P.S. Nicholson, J. Am. Ceram. Soc. 90 (2007) 1063–1070.
[22] G.C. Quan, K.T. Conlon, D.S. Wilkinson, J. Eur. Ceram. Soc. 27 (2007) 389–396.
[23] O. Lourie, H.D. Wagner, Compos. Sci. Technol. 59 (1999) 975–977.
[24] S.K. Pandey, O.P. Thakur, D.K. Bhattacharya, C. Prakash, R. Chatterjee, J. Alloys Compd. 468 (2009) 356–359.
[25] Z.P. Yang, X.L. Chao, C. Kang, R. Zhang, Mater. Res. Bull. 43 (2008) 38–44.
[26] W. Nhuapeng, T. Tunkasiri, J. Am. Ceram. Soc. 85 (2002) 700–702.
[27] Y. Wu, T. Feng, J. Alloys Compd. 491 (2010) 452–455.
[28] D.W. Wang, J.B. Jin, J. Yuan, B.L. Wen, Q.L. Zhao, D.Q. Zhang, M.S. Cao, Chin. Phys. Lett. 4 (2010) 047701.
[29] P.F. Becher, C.H. Hsueh, P. Angelini, T.N. Tiegs, J. Am. Ceram. Soc. 71 (1988) 1050–1061.
[30] Y. Waku, N. Nakagawa, T. Wakamoto, H. Ohtsubo, K. Shimizu, Y. Kohtoku, Nature 389 (1997) 49–52.
[31] C. Ionascu, R. Schaller, Mater. Sci. Eng. A 442 (2006) 175–178.
[32] T. Yamamoto, H. Igarashi, K. Okazaki, Ferroelectrics 63 (1985) 281–288.
[33] P.X. Gao, J. Song, J. Liu, Z.L. Wang, Adv. Mater. 19 (2007) 67–72.
[34] M.S. Cao, X.L. Shi, X.Y. Fang, Z.L. Hou, H.B. Jin, Y.J. Chen, Appl. Phys. Lett. 91 (2007) 203110.
[35] Y.N. Zhao, M.S. Cao, H.B. Jin, X.L. Shi, X. Li, S. Agathopoulos, J. Nanosci. Nanotechnol. 6 (2006) 2525–2528.
[36] M.S. Cao, X.L. Shi, X.Y. Fang, H.B. Jin, Z.L. Hou, W. Zhou, Appl. Phys. Lett. 91 (2007) 203110.
[37] M. Ristic, S. Music, M. Ivanda, S. Popovic, J. Alloys Compd. 397 (2005) L1–L4.
[38] S.R. Hejazi, H.R. Madaah Hosseini, M. Sasani Ghamsari, J. Alloys Compd. 455 (2008) 353–357.
[39] J.H. Yang, J.H. Zheng, H.J. Zhai, L.L. Yang, Y.J. Zhang, J.H. Lang, M. Cao, J. Alloys Compd. 475 (2009) 741–744.
[40] J.P. Cheng, Z.M. Liao, D. Shi, F. Liu, X.B. Zhang, J. Alloys Compd. 480 (2009) 741–746.
[41] X.Y. Gan, X.M. Li, X.D. Gao, W.D. Yu, J. Alloys Compd. 481 (2009) 397–401.
[42] X. Wu, P. Jiang, W. Cai, X.D. Bai, P. Goo, S.S. Xie, Adv. Eng. Mater. 10 (2008) 476–481.
[43] X. Wu, P. Jiang, Y. Ding, W. Cai, S.S. Xie, Z.L. Wang, Adv. Mater. 19 (2007) 2319–2322.
[44] H.B. Lin, M.S. Cao, Q.L. Zhao, X.L. Shi, D.W. Wang, F.C. Wang, Scripta Mater. 59 (2008) 780–783.
[45] Q.L. Zhao, M.S. Cao, J. Yuan, W.L. Song, R. Lu, D.W. Wang, D.Q. Zhang, J. Alloys Compd. 492 (2010) 264–268.
[46] H.B. Lin, M.S. Cao, J. Yuan, D.W. Wang, Q.L. Zhao, F.C. Wang, Chin. Phys. B 17 (2008) 4323–4327.
[47] Q.L. Zhao, M.S. Cao, J. Yuan, R. Lu, D.W. Wang, D.Q. Zhang, Mater. Lett. 64 (2010) 632–635.
[48] M.S. Cao, W. Zhou, X.L. Shi, Y.J. Chen, Appl. Phys. Lett. 91 (2007) 021912.
[49] Z.X. Guo, J. Xiong, M. Yang, W. Li, J. Alloys Compd. 461 (2008) 342–345.
[50] X. Zeng, A.L. Ding, T. Liu, G.C. Deng, X.S. Zheng, W.X. Cheng, J. Am. Ceram. Soc. 89 (2006) 728–730.
[51] C.W. Ahn, H.C. Song, S. Nahm, S. Priya, S.H. Park, K. Uchino, H.G. Lee, H.J. Lee, J. Am. Ceram. Soc. 89 (2006) 921–925.
[52] A. Banerjee, A. Bandyopadhyay, S. Bose, J. Am. Ceram. Soc. 89 (2006) 1594–1600.
[53] X.L. Chao, Z.P. Yang, X.H. Huang, D.F. Ma, J.H. Zeng, Curr. Appl. Phys. 9 (2009) 1283–1287.
[54] H. Li, Z.P. Yang, L.L. Wei, Y.F. Chang, Mater. Res. Bull. 44 (2009) 638–643.
[55] Y. Isogai, M. Miyayama, H. Yanagida, Sens. Actuators B 30 (1996) 47–53.
[56] R.C. Pohanka, S.W. Freiman, B.A. Bender, J. Am. Ceram. Soc. 61 (1978) 72–75.
[57] M. Ruhle, A.G. Evans, Prog. Mater. Sci. 33 (1989) 85–167.
[58] H.X. Zhai, Y. Huang, C.A. Wang, X. Wu, J. Am. Ceram. Soc. 83 (2000) 2006–2016.
[59] G. Ziegler, J. Heinrich, G. Wotting, J. Mater. Sci. 22 (1987) 3041–3086.
[60] A.D. Pabols, M.I. Osendi, P. Miranzo, Ceram. Int. 29 (2003) 757–764.
[61] Y. Zheng, B. Wang, C.H. Woo, Acta Mater. 56 (2008) 479–488.
[62] B. Zou, C.Z. Huang, M. Chen, M.L. Gu, H.L. Liu, Acta Mater. 55 (2007) 4193–4202.